ELSEVIER

Biophysical Chemistry 131 (2007) 105–110

Biophysical Chemistry

http://www.elsevier.com/locate/biophyschem

Atomic force microscope observation on biomembrane before and after peroxidation

Jin-Ye Wang [a,*], Li-Ping Wang [b], Qiu-Shi Ren [b]

[a] *Shanghai Institute of Organic Chemistry, Chinese Academy of Sciences, 354 Fenglin Road, Shanghai 200032, China*
[b] *School of Life Science and Biotechnology, Shanghai Jiaotong University, 1954 Huashan Road, Shanghai 200030, China*

Received 20 June 2007; received in revised form 25 September 2007; accepted 25 September 2007
Available online 2 October 2007

Abstract

Atomic force microscope (AFM) has been used to visualize the morphological change on the surface of erythrocyte membrane before and after oxidation. A smooth surface of intact erythrocyte cell was observed, while treatment by ferrous ion and ascorbate induced hemolysis of intact erythrocytes, generated many holes with average size of 146.6±33.2 nm in diameter (n=28) on membrane surface as seen by AFM. Ghost membrane and its inside-out vesicles were also used for the experiment. Skeleton structure and protein vesicles could be observed on the surface of an intact erythrocyte membrane before oxidation. Sendai virus induced fusion of inside-out vesicles seemed suppress peroxidation, while no such effect was observed in ghost membrane and erythrocyte systems.

Keywords: Asymmetry; Atomic force microscope; Erythrocyte; Fusion; Peroxidation; Sendai virus

1. Introduction

An asymmetric distribution of phospholipids between the inner and outer monolayer is a common feature of biological membranes [1]. Generally, most of phosphatidylcholine (PC) and sphingomyelin are distributed in the outer layer of the membrane, while phosphatidylethanolamine (PE) and phosphatidylserine (PS) in the inner layer of the membrane. Unlike membrane proteins, the asymmetric distribution of phospholipids is dynamically changed, which is called "flip-flop" and correlated with translocase [2–4]. Although the real physiological function of the asymmetric distribution is not very clear, it has been recognized that this is important for vesicular trafficking, including vesicle budding and fusion, molecular recognition and sorting between cells [5]. A direct evidence that PE as well as PS is exposed onto the cell surface during early stages of apoptosis, resulting in the total loss of asymmetric distribution of aminophospholipids in the plasma membrane bilayer has been proposed [6]. PE is redistributed at the cleavage furrow of dividing cells during cytokinesis, which may play a pivotal role in mediating a coordinate movement between the contractile ring and plasma membrane to achieve successful cell division [7]. On the other hand, membrane fusion is reported to stimulate phospholipid flip-flop between the external and internal monolayers, leading to a loss of membrane phospholipid asymmetry [8]. Another important rearrangement of phospholipids in biomembranes is bilayer-to-inverted hexagonal transition. Presence of the non-lamellar structures may be involved in membrane processes, either temporarily, like in membrane fusion or locally, e.g. to affect the activity of membrane-bound protein [9]. The fact that some amphiphiles which raise the bilayer to hexagonal phase transition temperature of PE inhibit Sendai virus-induced hemolysis of erythrocytes and fusion between ghosts and liposomes also implies the existence of nonbilayer intermediate [10]. We have shown in liposomal systems that the inverted hexagonal phase is more sensitive to hydroperoxidation than the multilamellar phase [11], and the higher content of aminophospholipid in the exofacial layer seems to be related with the higher rate of the

Abbreviations: AAPH, 2,2′-azobis (2-amidino-propane) dihydrochloride; AFM, atomic force microscope; MGO, DL-glycerin-monooleate; PC, phosphatidylcholine; PE, phosphatidylethanolamine; PS, phosphatidylserine; TBARS, thiobarbituric acid reactive substances; TNBS, 2, 4, 6-trinitrobenzenesulfonic acid.

* Corresponding author.
E-mail address: jywang@mail.sioc.ac.cn (J.-Y. Wang).

0301-4622/$ - see front matter © 2007 Elsevier B.V. All rights reserved.
doi:10.1016/j.bpc.2007.09.010

ferrous ion-induced peroxidation of multilamellar vesicles [12]. In the present study, human erythrocyte, which is a typical example that aminophospholipids distribute more in the inner leaflet, and its inside-out vesicles were used to compare the peroxidizability, as they have different amount of aminophospholipids in outer surface of the membrane. Erythrocytes fused by Sendai virus, ghosts fused by Sendai virus and lipid fusogen were also used for comparison with their unfused ones in ferrous ion induced peroxidation. Atomic force microscope (AFM) was used for observation of the membrane structure of both intact erythrocytes and ghost membranes before and after oxidation.

2. Experimental section

2.1. Materials

2, 4, 6-trinitrobenzenesulfonic acid (TNBS) was purchased from Sigma (St. Louis, MO, USA). Ferrous sulfate and other reagents such as antioxidants, buffers, organic solvents were of analytical grade.

2.2. Ghost membrane from human blood

Preparation was carried out at 4 °C. The fresh, heparinized human blood was centrifuged at 2000 ×*g* for 10 min, and erythrocytes were separated from plasma and buffy coat and washed three times in a physiological saline. White ghosts were prepared in phosphate buffer by the method of Steck and Kant with some modifications [13]. i.e., instead of alkaline buffer (pH 8.0) with lower concentration (5 mM), neutral buffer (pH 7.4) with a little higher concentration (10 mM) was used to prevent fragmentation of the ghost membranes. Half of the white ghost was further treated by the buffer with lower ion strength (0.5 mM, pH 8.0) to prepare inside-out vesicles [13]. Procedures of density barrier and ultracentrifugation were omitted. The concentration of the membrane was confirmed by phosphorus determination [14] after transferred the phosphate buffer into a physiological saline solution.

2.3. Membrane asymmetry analysis

Asymmetry of aminophospholipids in ghost membranes was investigated by TNBS labeling method [15]. Briefly, freshly prepared 0.01 M TNBS in the same buffer as membranes was added to the membrane solution in the presence or absence of 2% Triton X 100. The final concentration of TNBS was 0.6 mM. The reaction mixture was incubated at room temperature in the dark for 1 hour. Absorbance at 420 nm was analyzed.

2.4. Peroxidation analysis

Thiobarbituric acid reactive substances (TBARS) in ghost membrane and its inside-out vesicles were quantified by measuring malonyldiadehyde-thiobarbituric acid adducts formed by acid hydrolysis in boiling water for 15 min and then immediately cooled. After centrifuged at 8000 rpm for 5 min, absorbance at 535 nm was measured [16]. Oxygen consumption was monitored polarographically with a Clark-type oxygen probe (Rank Brothers, Cambridge, England). An incubation vessel, containing about 1.5 ml of membrane solution, was equipped with a magnetic stirrer, and the temperature was maintained at 37 °C in a circulating water bath. The solution was saturated with air prior to the addition of ferrous sulfate.

2.5. Fatty acid analysis

Total lipids were extracted from the ghost membrane by the method of Folch et al. [17]. Organic solvent (chloroform–methanol 2:1 by volume) contained 0.0002% of t-butyl hydroxyanisole as an antioxidant and a proper amount of heptadecanoic acid as an internal standard. Methyl esters of total lipids were prepared with 0.6 N methanolic–HCl as described by Kates [14]. Separation of fatty acid methyl esters was performed using a fused silica HR-SS-10 capillary column (25 m × 0.25 mm I.D.; Shinwa, Kyoto, Japan) with a splitless mode (Shimadzu GC 18A). Helium was used as a carrier gas. The initial oven temperature was 50 °C, increased to 160 °C at 20 °C /min, followed by an increase in temperature to 210 °C at 2 °C /min and then held constant for 10 min. The injector and detector temperature was 250 °C.

2.6. Atomic force microscope observation of biomembranes

Erythrocyte cells before and after oxidation with ferrous ion was diluted to about 2×10^5 cells/ml, fixed with 5% glutaraldehyde for 5 min (post fixation with 1% OsO_4 was needed for ghost membranes), deposited on a poly-lysine treated cover glass for adsorption of the cells. The extra solution was removed with filter paper, then a drop of sodium cacodylate buffer (20 mM, pH 7.4, 80 mg dextran 60C/ml, dextran can prevent the hemolysis of erythrocytes derived from washing) was added to wash and to remove sodium chloride of the sample, as sodium chloride will crystallize after drying the sample and disturb the observation. Subsequently most of the solution was removed by filter paper. The glass coverslip with attached cells was glued to a steel disc and placed on the stage of the atomic force microscope (AFM). AFM observation was carried out with Olympus OMPM-AFM-01 by a constant height mode in the air at room temperature. The sample was scanned under a sharpened pyramidal tip (silicon nitride) with a diameter of 40 nm (Olympus OMCL-TR400PS-2). The scan speed was 0.2 s/line. The size of holes on the membrane surface was randomly measured in the AFM image with Image-Pro Discovery Version 4.5 (Media Cybernetics Inc., USA).

2.7. Fusion with Sendai virus

Sendai virus (Z strain) was obtained kindly from Dr. Y. Kaneda, Osaka University, and grown in allantoic sac of embryonated chicken eggs (10-day old) and harvested after an 84 h incubation at 36 °C. After purification, hemagglutinating units (HAU) was measured against chicken erythrocytes. The mixture of erythrocytes and Sendai virus was first incubated at 4 °C for 10 min to allow agglutination, then moved to 37 °C and

Table 1
Distribution of aminophospholipids in external leaflet of ghost membranes and its inside-out vesicles and their oxygen consumptions induced by ferrous ion (0.1 mM) or AAPH (12.5 mM)

	A_{total} ($A_{420\ nm}$)	$A_{external}$ ($A_{420\ nm}$)	External/total (%)	O_2 consumption (nmol O_2/μmol P·min)	
				Fe^{2+}	AAPH
Inside-out Vesicles	0.462±0.003	0.419±0.008	90.7	36.56±6.43 *	15.53±0.54
Ghost Membrane	0.718±0.063	0.520±0.018	72.4	7.09±1.44 *	16.04±4.11

Oxygen consumption was monitored polarographically with a Clark-type oxygen probe (n=3).
* Represents the significant difference at $P<0.05$.

started the reaction with ferrous ion. Fusion was estimated with a phase-contrast microscope (Nikon). Fusion-induced hemolysis was determined by measuring the supernate's absorbance at 540 nm. Ghost membranes and inside-out vesicles were treated with Sendai virus as erythrocytes. Lipid fusogen, DL-glycerin-monooleate (MGO) induced fusion was carried out by including MGO in the sodium cacodylate buffer (20 mM, pH 7.4) at 175 μg/ml.

3. Results and discussion

The percentage of aminophospholipids distributed in the outer leaflet of inside-out vesicles was much higher than that in ghost membranes as expected, which was 91% for inside-out vesicles and 72% for ghost membranes (Table 1). In intact erythrocytes, only one-fifth of PE is present in the outer surface of the membrane when phospholipases are used to detect the distribution of phospholipids [18]. The asymmetry of ghost membrane used in present study should be lost partially as thirty volumes of hyposonic buffer was used for hemolysis of packed blood cells [19]. Moreover, our result of 72% was obtained by TNBS method. It has been indicated that variations of the order of 10% exist between the different laboratories with different techniques [20]. When carrying out these experiments, an implicit and sometimes unjustified assumption is that the lipid topology is stable over the reaction time and can resist membrane perturbations such as attack by exogenous phospholipases. Clearly, in the case of fast flip-flop, some of these techniques are no longer valid. Also, if lipid asymmetry is the result of a subtle balance between various lipid fluxes, membrane isolation is likely to lead to erroneous results. This is particularly true for the membranes of organelles.

Table 2
Comparison of oxygen consumption before and after fusion of human erythrocytes (10^8 cells/ml) with Sendai virus (320 HAU/ml), ghosts and their inside-out vesicles with Sendai virus/DL−glycerin−monooleate (MGO, 0.175 mg/ml)

	O_2 Consumption (nmol O_2/μmol P·min)	
	Fe^{2+} (0.1 mM)	(0.25 mM)
Erythrocytes		
With Sendai virus	22.10±2.68	
Without Sendai virus	18.31±4.47	
Ghost membrane		
With Sendai Virus		15.16±3.57
Without Sendai virus		14.78±2.33
Inside-out vesicles		
With Sendai virus		35.36±3.57*
Without Sendai Virus		80.38±2.06*
With MGO		47.67±14.74
Without MGO		56.20±9.82

*Represents the significant difference at $P<0.05$.

Oxygen consumption induced by ferrous ion in inside-out vesicles was more prominent than in ghosts as indicated in Table 1. TBARS assay showed that the absorbance at 535 nm was 0.022 per 0.118 μmol phospholipid for ghost membrane and 0.005 per 0.117 μmol phospholipid for inside-out vesicles before oxidation treatment. We can say that the result in Table 1 was not induced from the initial difference in phospholipid oxidation state of the membranes. On the other hand, there was no prominent difference in oxygen consumption when 2,2′-azobis (2-amidino-propane) dihydrochloride (AAPH) was used as a radical inducer. These results were consistent with our previous study in liposomal system, and also with our recent result for rat erythrocytes [12,21], which can be explained as the higher distribution of amino phospholipids in the outer leaflet of the membrane. Besides asymmetric distribution of PC and PE in biomembranes, they constitute very heterogeneous classes of phospholipids represented by various molecular species which differ in the structure and composition of their fatty acids. PE always contains more amount of polyunsaturated fatty acids than PC in biomembranes such as erythrocytes, which results in the external monolayer being more tightly packed and less fluid than the internal monolayer [22,23]. But more proportion of polyunsaturated fatty acids in aminophospholipids of the ghost membrane is difficult to interpret the different result between ferrous ion and AAPH induced peroxidation. Amino groups may also be accounted for the higher susceptibility of the inside-out vesicles.

Pre-incubation of erythrocytes at 4 °C for 10 min in the presence and absence of Sendai virus corresponded a slight hemolysis. Fusion did not occur at this step. But this process was necessary for starting the fusion immediately after moved the mixture to 37 °C [24]. Fusion is considered to commence and precede hemolysis in this case, as low concentration of virus was used [25]. As indicated in Table 2, no significant difference in oxygen consumption between fused and unfused erythrocytes, although structural change of phospholipids in membranes was expected. Actually, intact erythrocytes were quite difficult to be oxidized. If we increased the dose of ferrous ion to 0.25 mM (final concentration), there was more oxygen consumption in Sendai virus-induced fused erythrocytes than unfused ones (68.19 nmol O_2/μmol P· min to 50.01 nmol O_2/μmol P· min), but the hemolysis was also increased. As ferrous ion can be released from hemoglobin during hemolysis [26], it

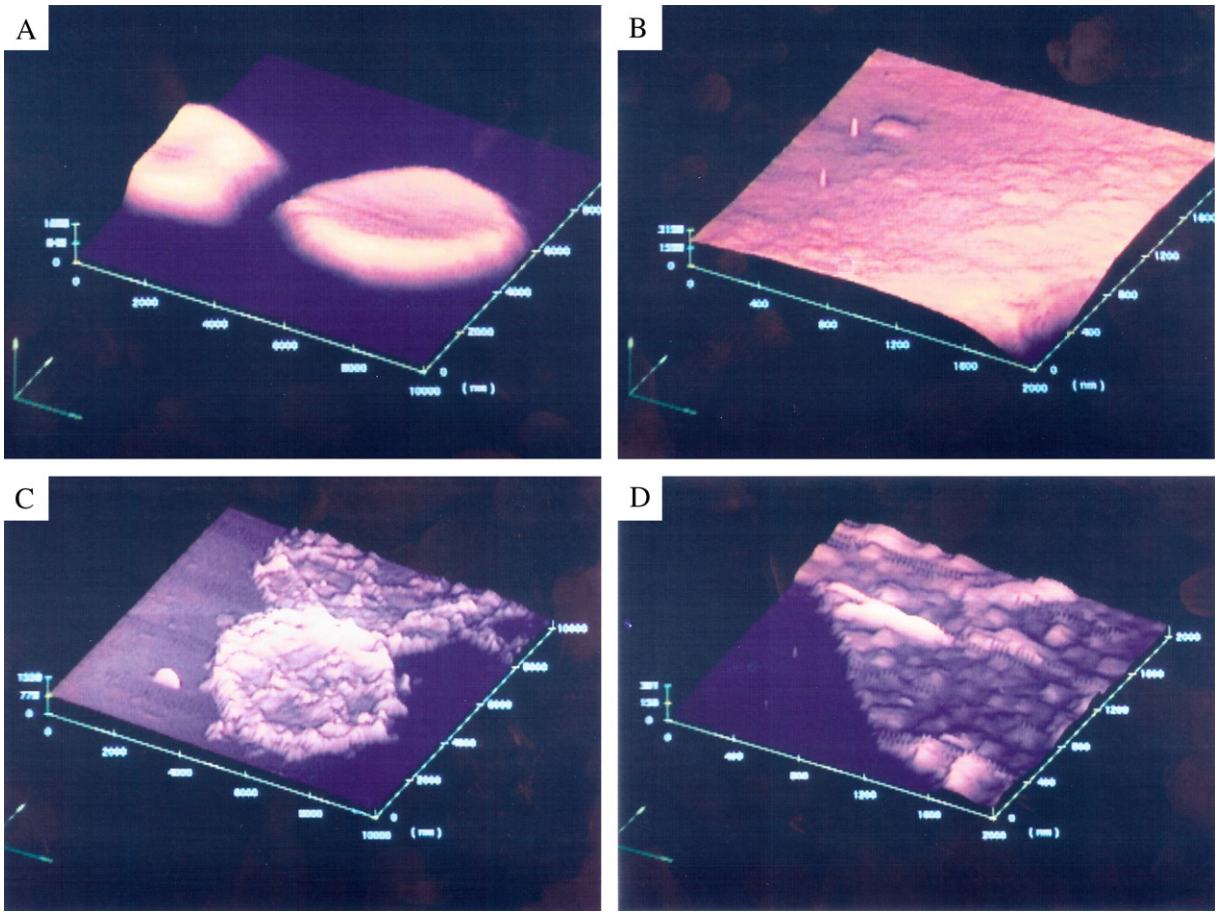

Fig. 1. Three-dimensional AFM images of intact erythrocytes (A, B) and ghost membranes (C, D). A and C, scanning area 10×10 μm^2; B and D, scanning area 0.2×0.2 μm^2.

was difficult to estimate if the difference of oxygen consumption was derived from fusion or hemolysis.

Such problem can be avoided by using ghost membranes. However, by incubation of inside-out vesicles with Sendai virus, a mysterious result was obtained. Oxygen consumption of fused inside-out membranes was much less than unfused ones. i.e., fusion by Sendai virus inhibited the ferrous ion induced oxidation. On the other hand, there was no such difference in ghost membranes (Table 2). As shown in Table 1, Over 90% of aminophospholipids distributed in the outer surface of the inside-out vesicles. This kind of asymmetry of distribution of aminophospholipids, which has a very high levels of unsaturated acyl chains in the outer monolayer, is reverse to erythrocyte membranes, and may be a more suitable target for virus-induced fusion [27]. The possible explanation on our result is that fusion leads to a loss of membrane phospholipid asymmetry and a decrease of aminophospholipids distributed in the membrane surface in inside-out vesicles [8], and furthermore lowers the oxidation susceptibility of the membranes. On the other hand, there was no significant change in aminophospholipids distribution in ghost membranes before and after fusion, as the ghost membranes are more symmetric. Different from Sendai virus-induced fusion, incubation of inside-out vesicles with and without MGO did not show significant difference in oxygen consumption. MGO contains oleate which has been reported to reduce oxidation of liposomes by a direct "antioxidant"-like effect [28]. MGO, besides its function as a fusogen, may also play a role in prevention of oxidation of ghost membranes by ferrous ion. ^{31}P-NMR has shown the existence of inverted hexagonal phase during fusion of human erythrocyte ghosts induced by MGO [29], effect of the inverted hexagonal on peroxidizability of ghost membranes may be deleted by the antioxidant-like effect of MGO.

Atomic force microscope (AFM) has emerged in ultrastructural biology as a broadly used tool capable to provide a quantitative description of morphological details of rugged cell exterior or biomolecular assemblies under physiological and non-physiological conditions (e.g., dried or chemically fixed samples). The key features of the membrane skeleton of the erythrocyte and height information on the skeletal components with unprecedented accuracy has been identified using ghost membranes [30,31], which was consistent with that observed by negative stain transmission electron microscope (TEM) [32]. The spread meshwork reveals the hexagonal lattice of junctional complexes, containing short F-actin and band 4.1, cross-linked by spectrin filaments. While for those intact erythrocytes, only particles above the cell surface could be observed by AFM [33]. In this study, we tried to visualize the morphological change on the surface of erythrocyte membranes during peroxidation. A smooth surface of intact erythrocyte cells was observed

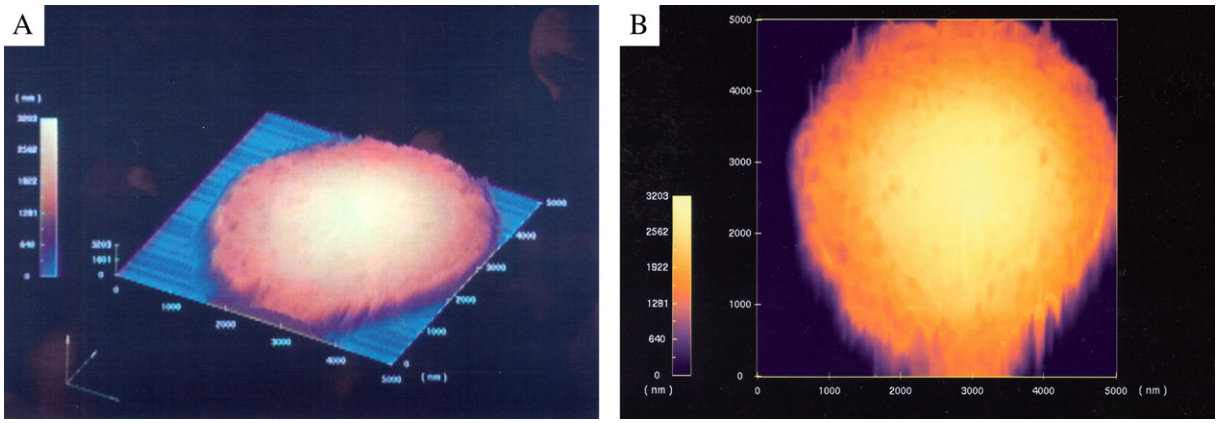

Fig. 2. AFM images of intact erythrocytes after oxidation by ferrous ion for 30 min. A, three-dimensional AFM images, scanning area 5×5 μm^2; B, top view of A showing many holes on the cell surface due to oxidation derived hemolysis.

(Fig. 1A, B), the cell packed a little in the center of its biconcave shape, and had about 6 μm in diameter. Treatment by ferrous ion and ascorbate generated many holes with various sizes on membrane surface (146.6±33.2 nm in diameter, n=28, Fig. 2), which might result in leakage of proteins and other molecules from cells, and decrease of the cell size. Proper concentration of ascorbate (~20 mM) could reduce iron-catalyzed hydrogen peroxide induced peroxidation of erythrocyte membranes, but both ascorbate and iron could stimulate lysis of erythrocytes [34,35]. We also considered the possibility that the hemolysis, not the peroxidation, might attribute to the formation of these holes under the experimental condition (monitored by the increase of absorbance at 540 nm for 30 min of incubation at 37 °C). But the result by TEM observation did not support the assumption (data not shown). Although it has been known that AFM has a merit for observation of biological samples under physiological condition, it is still difficult to get surface structure with high resolution by keeping cells in normal shapes. We tried various washing buffers and found that the fine membrane structure could be observed by using intact erythrocyte cells after treatment with sodium cacodylate buffer (20 mM, pH 7.4, 80 mg dextran 60C/ml). As sodium chloride in buffer will crystallize after drying the sample and disturb the observation, washing is necessary. Dextran can prevent the hemolysis of erythrocytes derived from washing. In the present work, glutaraldehyde fixed erythrocytes were imaged by AFM in constant height mode under air-dried condition. Fixation is necessary, because high-resolution images of cells are hardly achieved in solution. The softness of erythrocyte membranes and thermal fluctuation make the cells move and deform when the cells were tapped for scanning. It has been confirmed that the fixation does not alter the topographic features of the cell surface, though the particles observed might be slightly larger due to the expansion effect of glutaraldehyde, which induces some slight conformational changes of the proteins [36]. Fig. 3B showed the skeleton structure and protein vesicles on the surface of erythrocyte cells. The length of filaments connecting protein vesicles was 100–200 nm, which was consistent with the reported result by negative stain transmission electron microscope [32]. It should be noted that this fine structure could

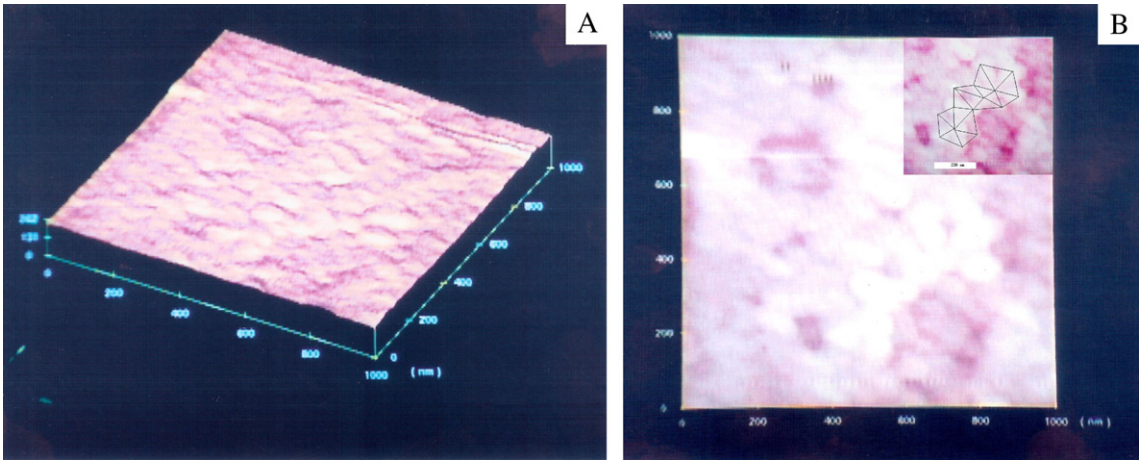

Fig. 3. AFM image of the surface structure of an intact erythrocyte cell washed with sodium cacodylate buffer (20 mM, pH 7.4, 80 mg dextran 60 °C/ml). A, three-dimensional representation of the cell surface, scanning area 1000×1000 nm^2; B, top view of A showing networklike structures and protein vesicles with diameter of 62.1±10.9 nm (n=30). Insert is the image of further enlargement of surface texturing, additional network of black lines linking protein vesicles is added as our interpretation of the features of the intact membrane-skeletal network showing lengths consistent with ~200 nm contours (bar is 200 nm).

only be distinguished in top view, but not in three-dimensional representation (Fig. 3A is the same image as B).

In conclusion, due to asymmetric structure of erythrocyte membranes, difference in amount of aminophospholipids distributed in out monolayer of membranes or change of the distribution induced by fusion will affect the susceptibility of the membranes against ferrous ion induced peroxidation.

Acknowledgement

This study was partly supported by the National Program on Key Basic Research Projects of China (973 Program, 2005CB724306), the National Natural Science Foundation of China (30270365, 30470477).

References

[1] A. Zachowski, Phospholipids in animal eukaryotic membranes: transverse asymmetry and movement, Biochem. J. 294 (2003) 1–41.
[2] X. Tang, M.S. Halleck, R.A. Schlegel, P. Williamson, A subfamily of P-type ATPases with aminophospholipid transporting activity, Science 272 (1996) 1495–1497.
[3] A. van Helvoort, A.J. Smith, H. Sprong, I. Fritzsche, A.H. Schinkel, P. Borst, G. van Meer, MDR1 P-glycoprotein is a lipid translocase of broad specificity, while MDR3 P-glycoprotein specifically translocates phosphatidylcholine, Cell 87 (1996) 507–517.
[4] Q. Zhou, J. Zhao, J.G. Stout, R.A. Luhm, T. Wiedmer, P.J. Sims, Molecular cloning of human plasma membrane phospholipid scramblase. A protein mediating transbilayer movement of plasma membrane phospholipids, J. Biol. Chem. 272 (1997) 18240–18244.
[5] P.F. Devaux, Static and dynamic lipid asymmetry in cell membranes, Biochemistry 30 (1991) 1163–1173.
[6] K. Emoto, N. Toyama-Sorimachi, H. Karasuyama, K. Inoue, M. Umeda, Exposure of phosphatidylethanolamine on the surface of apoptotic cells, Exp. Cell Res. 232 (1997) 430–434.
[7] K. Emoto, T. Kobayashi, A. Yamaji, H. Aizawa, I. Yahara, K. Inoue, M. Umeda, Redistribution of phosphatidylethanolamine at the cleavage furrow of dividing cells during cytokinesis, Proc. Natl. Acad. Sci. U. S. A. 93 (1996) 12867–12872.
[8] P. Comfurius, J.M. Senden, R.H. Tilly, A.J. Schroit, E.M. Bevers, R.F. Zwaal, Loss of membrane phospholipid asymmetry in platelets and red cells may be associated with calcium-induced shedding of plasma membrane and inhibition of aminophospholipid translocase, Biochim. Biophys. Acta 1026 (1990) 153–160.
[9] K. Lohner, Is the high propensity of ethanolamine plasmalogens to form non-lamellar lipid structures manifested in the properties of biomembranes? Chem. Phys. Lipids 81 (1996) 167–184.
[10] J.J. Cheetham, S. Nir, E. Johnson, T.G. Flanagan, R.M. Epand, The effects of membrane physical properties on the fusion of Sendai virus with human erythrocyte ghosts and liposomes. Analysis of kinetics and extent of fusion, J. Biol. Chem. 269 (1994) 5467–5472.
[11] J.Y. Wang, T. Miyazawa, K. Fujimoto, Z.Y. Wang, T. Nozawa, The inverted hexagonal phase is more sensitive to hydroperoxidation than the multilamellar phase in phosphatidylcholine and phosphatidylethanolamine aqueous dispersions, FEBS Lett. 310 (1992) 106–110.
[12] J.Y. Wang, Z.Y. Wang, T. Kouyama, T. Shibata, T. Ueki, Significance of amino groups of phosphatidylethanolamine in phospholipid peroxidation of mixed liposomes, Chem. Phys. Lipids 71 (1994) 197–203.
[13] T.L. Steck, J.A. Kant, Preparation of impermeable ghosts and inside-out vesicles from human erythrocyte membranes, Methods Enzymol. 31 (1974) 172–180.
[14] M. Kates, In Techniques of Lipidology Amsterdam: Elsevier Science (1986), pp. 113-115, pp. 248-250.
[15] P. Sarti, A. Molinari, G. Arancia, A. Meloni, G. Citro, A modified spectroscopic method for the determination of the transbilayer distribution of phosphatidylethanolamine in soya-bean asolectin small unilamellar vesicles, Biochem. J. 312 (1995) 643–648.
[16] J.A. Buege, S.D. Aust, Microsomal lipid peroxidation, Methods Enzymol. 52 (1978) 302–310.
[17] J. Folch, M. Lees, G.H. Sloane-Stanley, A simple method for the isolation and purification of total lipides from animal tissues, J. Biol. Chem. 226 (1957) 497–509.
[18] A.J. Verkleij, R.F.A. Zwaal, B. Roelofsen, P. Comfurius, D. Kastelijn, L.L.M. van Deenen, Asymmetric distribution of phospholipids in the human red cell membrane. Combined study using phospholipases and freeze-etch electron microscopy, Biochim. Biophys. Acta 323 (1973) 178–193.
[19] P. Williamson, L. Algarin, J. Bateman, H.R. Choe, R.A. Schlegel, Phospholipid asymmetry in human erythrocyte ghosts, J. Cell. Physiol. 123 (1985) 209–214.
[20] P.F. Devaux, Static and dynamic lipid asymmetry in cell membranes, Biochemistry 30 (1991) 1163–1173.
[21] L. Di, W. Liu, Y. Liu, J.Y. Wang, Effect of asymmetric distribution of phospholipids in ghost membrane from rat blood on peroxidation induced by ferrous ion, FEBS Lett. 580 (2006) 685–690.
[22] W.E. Connor, D.S. Lin, G. Thomas, F. Ey, T. DeLoughery, N. Zhu, Abnormal phospholipid molecular species of erythrocytes in sickle cell anemia, J. Lipid Res. 38 (1997) 2516–2528.
[23] G. Morrot, S. Cribier, P.F. Devaux, D. Geldwerth, J. Davoust, J.F. Bureau, P. Fellmann, P. Herve, B. Frilley, Asymmetric lateral mobility of phospholipids in the human erythrocyte membrane, Proc. Natl. Acad. Sci. U. S. A. 83 (1986) 6863–6867.
[24] Y. Okada, Sendai virus-induced cell fusion, Methods Enzymol. 221 (1993) 18–41.
[25] H. Peretz, Z. Toister, Y. Laster, A. Loyter, Fusion of intact human erythrocytes and erythrocyte ghosts, J. Cell Biol. 63 (1974) 1–11.
[26] T. Ito, M. Nakano, Y. Yamamoto, T. Hiramitsu, Y. Mizuno, Hemoglobin-induced lipid peroxidation in the retina: a possible mechanism for macular degeneration, Arch. Biochem. Biophys. 316 (1995) 864–872.
[27] A. Herrmann, M.J. Clague, A. Puri, S.J. Morris, R. Blumenthal, S. Grimaldi, Effect of erythrocyte transbilayer phospholipid distribution on fusion with vesicular stomatitis virus, Biochemistry 29 (1990) 4054–4058.
[28] C. Lee, J. Barnett, P.D. Reaven, Liposomes enriched in oleic acid are less susceptible to oxidation and have less proinflammatory activity when exposed to oxidizing conditions, J. Lipid Res. 39 (1998) 1239–1247.
[29] M.J. Hope, P.R. Cullis, The role of nonbilayer lipid structures in the fusion of human erythrocytes induced by lipid fusogens, Biochim. Biophys. Acta 640 (1981) 82–90.
[30] A.H. Swihart, J.M. Mikrut, J.B. Ketterson, R.C. Macdonald, Atomic force microscopy of the erythrocyte membrane skeleton, J. Microsc. 204 (2001) 212–225.
[31] H. Takeuchi, H. Miyamoto, Y. Sako, H. Komizu, A. Kusumi, Structure of the erythrocyte membrane skeleton as observed by atomic force microscopy, Biophys. J. 74 (1998) 2171–2183.
[32] S.C. Liu, L.H. Derick, J. Palek, Visualization of the hexagonal lattice in the erythrocyte membrane skeleton, J. Cell Biol. 104 (1987) 527–536.
[33] M. Girasole, G. Pompeo, A. Cricenti, A. Congiu-Castellano, F. Andreola, A. Serafino, B.H. Frazer, G. Boumis, G. Amiconi, Roughness of the plasma membrane as an independent morphological parameter to study RBCs: a quantitative atomic force microscopy investigation, Biochim. Biophys. Acta 1768 (2007) 1268–1276.
[34] H. Einsele, M.R. Clemens, H. Remmer, Effect of ascorbate on red blood cell lipid peroxidation, Free Radic. Res. Commun. 1 (1985) 63–67.
[35] R.A. Lovstad, Ascorbate and dehydroascorbate stimulation of copper induced hemolysis. Protective action of ceruloplasmin, albumin and apotransferrin, Int. J. Biochem. 16 (1984) 155–159.
[36] P.C. Zhang, C.L. Bai, Y.M. Huang, H. Zhao, Y. Fang, N.X. Wang, Q. Li, Atomic force microscopy study of fine structures of the entire surface of red blood cells, Scanning Microsc. 9 (1995) 981–988.